JACS
JOURNAL OF THE AMERICAN CHEMICAL SOCIETY
Article
pubs.acs.org/JACS

Reductive Elimination of H_2 Activates Nitrogenase to Reduce the N≡N Triple Bond: Characterization of the E_4(4H) Janus Intermediate in Wild-Type Enzyme

Dmitriy Lukoyanov,[†] Nimesh Khadka,[‡] Zhi-Yong Yang,[‡] Dennis R. Dean,[§] Lance C. Seefeldt,*[,‡] and Brian M. Hoffman*[,†]

[†]Departments of Chemistry and Molecular Biosciences, Northwestern University, Evanston, Illinois 60208, United States
[‡]Department of Chemistry and Biochemistry, Utah State University, Logan, Utah 84322, United States
[§]Department of Biochemistry, Virginia Tech, Blacksburg, Virginia 24061, United States

ABSTRACT: We proposed a reductive elimination/oxidative addition (*re*/*oa*) mechanism for reduction of N_2 to $2NH_3$ by nitrogenase, based on identification of a freeze-trapped intermediate of the α-$70^{Val\rightarrow Ile}$ MoFe protein as the Janus intermediate that stores four reducing equivalents on FeMo-co as two [Fe−H−Fe] bridging hydrides (denoted E_4(4H)). The mechanism postulates that obligatory *re* of the hydrides as H_2 drives reduction of N_2 to a state (denoted E_4(2N2H)) with a moiety at the diazene (HN═NH) reduction level bound to the catalytic FeMo-co. EPR/ENDOR/photophysical measurements on wild type (WT) MoFe protein now establish this mechanism. They show that a state freeze-trapped during N_2 reduction by WT MoFe is the same Janus intermediate, thereby establishing the α-$70^{Val\rightarrow Ile}$ intermediate as a reliable guide to mechanism. Monitoring the Janus state in WT MoFe during N_2 reduction under mixed-isotope condition, H_2O buffer/D_2, and the converse, establishes that the bridging hydrides/deuterides do not exchange with solvent during enzymatic turnover, thereby solving longstanding puzzles. Relaxation of E_4(2N2H) to the WT resting-state is shown to occur via *oa* of H_2 and release of N_2 to form Janus, followed by sequential release of two H_2, demonstrating the kinetic reversibility of the *re*/*oa* equilibrium. Relative populations of E_4(2N2H)/E_4(4H) freeze-trapped during WT turnover furthermore show that the reversible *re*/*oa* equilibrium between [E_4(4H) + N_2] and [E_4(2N2H) + H_2] is ∼ thermoneutral ($\Delta_{re}G^0$ ∼ −2 kcal/mol), whereas, by itself, hydrogenation of $N_2(g)$ is highly endergonic. These findings demonstrate that (i) *re*/*oa* accounts for the historical *Key Constraints* on mechanism, (ii) that Janus is central to N_2 reduction by WT enzyme, which (iii) indeed occurs via the *re*/*oa* mechanism. Thus, emerges a picture of the central mechanistic steps by which nitrogenase carries out one of the most challenging chemical transformations in biology.

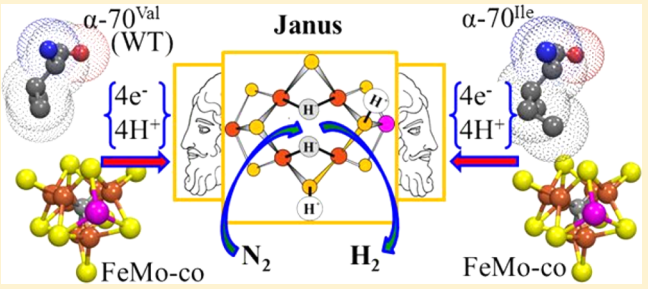

INTRODUCTION

By catalyzing biological nitrogen fixation—the reduction of N_2 to two NH_3 molecules—nitrogenase generates the nitrogen-containing nutrients that support most of the biosphere, including over half the human population.[1] But an understanding of the mechanism of N_2 reduction by nitrogenase has been elusive. A "kinetic" foundation for the mechanism of the Mo-dependent nitrogenase was developed through extensive studies in the 1970s and 1980s.[2−4] The culmination of these measurements was the Lowe−Thorneley (LT) kinetic scheme for nitrogenase function, Figure 1,[2−4] which describes the transformations among catalytic intermediates, denoted E_n where n is the number of electrons/protons delivered from the nitrogenase Fe protein to the MoFe protein, which contains the active site iron−molybdenum cofactor ([7Fe-9S-Mo-C-*R*-homocitrate, denoted **M**]; FeMo-co) Figure 2. A defining feature of this scheme is the obligatory formation of one mole of H_2 per mole of N_2 reduced, which leads to a limiting

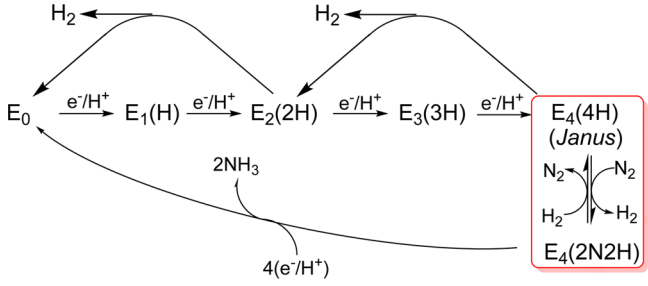

Figure 1. Simplified Lowe−Thorneley (LT) kinetic scheme for nitrogen reduction[2−4] that focus on the electron-accumulation and FeMo-co activation (boxed) stages. In the E_n notation, n = number of [e^-/H^+] added to FeMo-co.

Received: June 20, 2016
Published: August 16, 2016

DOI: 10.1021/jacs.6b06362
J. Am. Chem. Soc. 2016, 138, 10674−10683

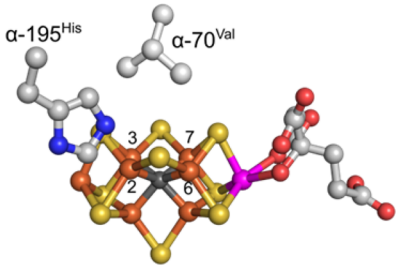

Figure 2. Crystal structure of FeMo-co. Fe is shown in rust, Mo in magenta, S in yellow, carbide in dark-gray, carbon in gray, N in blue and O in red. The Fe atoms of catalytic 4Fe-4S face are labeled as 2, 3, 6, and 7. Two amino acids, α-70^{Val} and α-195^{His}, that approach the FeMo-co are also shown. The image was created using PDB coordinate 2AFI.

stoichiometry for enzyme-catalyzed nitrogen fixation given by eq 1,

$$N_2 + 8e^- + 16\,ATP + 8H^+ \rightarrow 2NH_3 + H_2 + 16\,ADP + 16\,P_i \quad (1)$$

in agreement with stoichiometric measurements by Simpson and Burris.[5] However, the obligatory requirement for H_2 formation has not been universally accepted, and was even questioned in the culminating review of Burgess and Lowe: "Thus, the data that support the obligatory evolution of one H_2 for every N_2 reduced are much less compelling than the data that require us to believe that some H_2 will always be evolved during N_2 reduction."[2]

We recently proposed[6,7] that obligatory H_2 formation during nitrogenase N_2 reduction is in fact required to explain the catalytic function of nitrogenase. This proposal originates with the characterization of an intermediate (FeMo-co spin $S = 1/2$) trapped during turnover of MoFe protein having the α-70$^{Val\rightarrow Ile}$ substitution, which apparently inhibits access by all substrates to the active site, other than protons.[8] A combination of $^{1,2}H/^{95}Mo$ ENDOR spectroscopy[8,9] and cryoannealing "electron counting"[10] showed this state to be the key $E_4(4H)$ "Janus" intermediate, which has accumulated four of the eight reducing equivalents required by eq 1, storing them as two [Fe−H−Fe] bridging hydrides.[8−10] $E_4(4H)$ sits at a transition in the N_2 reduction pathway, Figure 1, poised to "fall back" to the E_0 resting state by successive release of two H_2,[10] but equally poised to eliminate H_2 and proceed to the reduction of N_2 to two NH_3 through the accumulation of four more equivalents, hence the appellation, "Janus".[7]

The discovery that the four reducing equivalents accumulated by $E_4(4H)$ are stored as bridging hydrides forged a connection between nitrogenase catalysis and the organometallic chemistry of metal hydrides[11−13] that offered explanations of a multitude of features of nitrogenase mechanism that had defied explanation for decades.[2] At the most basic level, this hydride formation helped to explain how a constant-potential electron donor, reduced Fe protein (Fe^{red}), could reduce FeMo-co by 4 equiv. Moreover, bridging hydrides are less susceptible to protonation to form H_2, or to solvent exchange, than terminal hydrides. As a consequence of the latter, bridging hydrides diminish the tendency of FeMo-co to "fall back" to resting state through the formation of two H_2 (Figure 1). However, the bridging mode also lowers hydride reactivity, relative to that of terminal hydrides. How the release of H_2 contributes to the activation of this "deactivated" intermediate for the hydrogenation of N_2 to a moiety at the N_2H_2-reduction level is thus a central "mystery" of N_2 reduction by nitrogenase.

Importantly, reference to the inorganic chemistry of metal-dihydrides offered an explanation to this mystery, as well. Once it is recognized that $E_4(4H)$ contains two bridging hydrides, then the chemistry of metal-dihydride complexes[11−13] identifies the LT $E_4(4H) \leftrightarrow E_4(2N2H)$ mechanistically coupled equilibrium (Figure 1) as the reductive elimination (*re*) of H_2 and its reverse, the oxidative addition (*oa*) of H_2, Figure 3. We

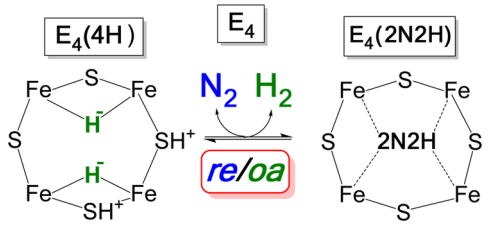

Figure 3. Schematic of *re*/*oa* Equilibrium. The cartoon represents the Fe 2,3,6,7 face of FeMo-co, and the "2N2H" implies a species at the diazene reduction level of unknown structure and coordination geometry. In the indicated equilibrium the binding and activation of N_2 is mechanistically coupled to the *re* of H_2, as described in the text. Some of the potential complexities associated with this enzymatic process that underlie this cartoon are discussed in ref 18.

proposed that for nitrogenase, the *re* of H_2 carries off two of the four reducing equivalents formally stored as the H^-, driving the first, and most difficult, step of N_2 cleavage: reduction of the N_2 triple bond to a diazene-level (2N2H) moiety bound to FeMo-cofactor, Figure 3, by the remaining two reducing equivalents. This process fulfills one of the long-standing *Key Constraints* on mechanism: Chart 1, (i).[2]

Chart 1. *Key Constraints* on Nitrogenase Mechanism[2]

(i) State when N_2 is Reduced:
N_2 is reduced at the E_4 stage of [e^-/H^+] accumulation

(ii) D_2 or T_2 only react during N_2 Turnover, during which:

(a) 2HD form stoichiometrically:
$\mathbf{M}\text{-}N_2 + D_2 + 2H^+ + 2e^- \Longrightarrow 2HD + \mathbf{M} + N_2$

(b) No Scrambling with solvent:
'No' T^+ released to solvent under T_2

(c) Reduction Level of this reaction:
D_2/T_2 reacts at $E_4(2N2H)$ level

The proposal that N_2 fixation requires the obligatory *re* of H_2 was first supported by its ability to provide explanations of key constraints on nitrogenase mechanism summarized in Chart 1.[2] These include not only the E_n state at which N_2 is first reduced (*Key Constraint* (i)), but most especially previously baffling results from turnover in the presence of D_2/T_2. It was found that (*Key Constraints* (ii)), D_2 only reacts with nitrogenase during turnover under an N_2/D_2 atmosphere; (ii)a in this reaction D_2 is stoichiometrically reduced to two HD (with H_2O buffer); (ii)b, corresponding turnover with T_2 does not lead to exchange of T^+ into H_2O solvent.[2] These constraints are explained as arising through the reverse of the *re* process, Figure 3, namely the oxidative addition (*oa*) of H_2 with loss of N_2.[6,7]

DOI: 10.1021/jacs.6b06362
J. Am. Chem. Soc. 2016, 138, 10674−10683

According to the mechanism, during turnover under D_2/N_2, reaction of the $E_4(2N2H)$ intermediate with D_2 generates dideutero-E_4 with two [Fe−D−Fe] bridging deuterides which do not exchange with solvent.[14] This $E_4(4H)$ isotopologue, which we denote $E_4(2D^-;2H^+)$ (Chart 2), would relax through $E_2(D^-;H^+)$ to E_0 with successive loss of two HD.[7,10]

Chart 2

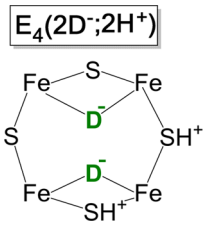

The proposed formation of the $E_4(2D^-;2H^+)$ and $E_2(D^-;H^+)$ states through the *thermodynamically* allowed reverse of *re*, the *oa* of D_2 with accompanying release of N_2, led to a successful test of their formation. During turnover under N_2/D_2, the nonphysiological substrate acetylene (C_2H_2) intercepted these states to generate deuterated ethylenes (C_2H_3D and $C_2H_2D_2$).[14] More recently, we identified an $S = 1/2$ EPR signal that appears during N_2 reduction by wild type (WT) MoFe protein as arising from FeMo-co of the $E_4(2N2H)$ state formed by *re* of H_2 with N_2 reduction, Figure 3, and in so doing confirmed the prediction that the (*re*/*oa*) activation equilibrium is not only thermodynamically, but also *kinetically* reversible.[15] Characterization of the $E_4(4H)$ "Janus" intermediate as carrying four reducing equivalents in the form of two [Fe−H−Fe] bridging hydrides thus laid the foundation for the *re*/*oa* mechanism, Figure 3, with its obligatory formation of one H_2 per N_2 reduced and resultant limiting stoichiometry of eq 1,[15] while the success of predictions based on the mechanism provides powerful support for the mechanism.

We here report two major *types* of advance in our understanding of nitrogenase catalysis. The *first* was motivated by our recognition that, although the predictions of *re*/*oa* were tested in WT MoFe, the mechanism was founded on the presence and properties of the two [Fe−H−Fe] bridging hydrides in the Janus intermediate trapped and characterized in the α-$70^{Val\rightarrow Ile}$ MoFe protein, which shows a much decreased ability to bind and reduce N_2. This raised the question: *Do the properties of the Janus intermediate in the MoFe variant accurately reflect those of the WT intermediate, and are mechanistic conclusions based on studies of the variant applicable to WT enzyme?* This report answers these coupled questions: yes. We here establish that the same $E_4(4H)$ Janus intermediate, with its two [Fe−H−Fe] bridging hydrides, in fact does participate in catalysis by the WT enzyme through the *re*/*oa* mechanism for N_2 reduction, thereby showing the α-$70^{Val\rightarrow Ile}$ Janus intermediate to be a reliable guide to mechanism.

The *second* type involves observations founded on the ability to monitor both the $E_4(4H)$ and $E_4(2N2H)$ partners of the *re*/*oa* equilibrium in WT enzyme (Figure 3). This ability enables us to experimentally demonstrate that the *re*/*oa* mechanism indeed satisfies the *Key Constraints* of Chart 1, and beyond that to measure the energetics and kinetics of the equilibrium interconversion. Overall, this report yields a picture of the key mechanistic steps by which nitrogenase carries out one of the most challenging chemical transformation in biology, the reduction of the N≡N triple bond.[16]

MATERIALS AND METHODS

Materials and Protein Purifications. All the reagents were obtained from SigmaAldrich (St. Louis, MO) or Fisher Scientific (Fair Lawn, NJ) and were used without further purification. Argon and N_2 gases were purchased from Air Liquide America Specialty Gases LLC (Plumsteadville, PA). Experiments were carried out with WT *Azotobacter vinelandii* MoFe protein expressed and purified as described elsewhere.[17] The handling of all buffers and proteins were done anaerobically unless stated otherwise.

EPR and ENDOR Samples. Samples were prepared as described under turnover conditions specified in figure legends; X-band samples contain 50 μM MoFe protein, 75 μM Fe protein, and the concentration of intermediates trapped during turnover is typically ~20 μM.[15,18] For Q-band samples, 100 μM MoFe and 150 μM Fe was used. All the samples were allowed to turnover for 20−25s, transferred to a X or Q-band tube, and frozen with liquid nitrogen.[15,18] It was found that during turnover of WT enzyme under low partial pressures of N_2 a $g_1 = 2.15$ species, shown below to be the $E_4(4H)$ intermediate in WT enzyme could be trapped in populations adequate for study, typically along with its "equilibrium partner" the $E_4(2N2H)$ intermediate. The properties of $g_1 = 2.15$, $E_4(4H)$ are compared with those of $E_4(4H)$ trapped in the α-$70^{Val\rightarrow Ile}$ and α-$70^{Val\rightarrow Ile}$/α-$195^{His\rightarrow Gln}$ MoFe proteins as described.[17,18]

EPR and ENDOR Measurements. X-band CW EPR spectra and Q-band CW EPR and ^{1,2}H ENDOR spectra, including those during in situ photolysis by constant 450 nm diode laser illumination, were collected as described.[18] Data points for kinetics of photolysis and annealing were obtained as amplitudes of EPR signals at the well-resolved g_1 features of the E_4 states linked by *re*/*oa*. Tests of this protocol by EPR simulations show that the error of this quantitation approach should not exceed 15% when both $E_4(4H)$ and $E_4(4D)$ intermediates are present. We recall a time constant for photolysis is inversely proportional to the intensity of illumination and photolysis quantum yield.[18] As a result the kinetic isotope effect on photolysis corresponds to the effect on quantum yield.

RESULTS AND DISCUSSION

Enhancing the Population of the WT $g_1 = 2.15$ Intermediate. Figure 4 presents EPR spectra of WT MoFe protein freeze-quenched under turnover at high and low partial pressure of N_2, along with a spectrum of the $E_4(4H)$ intermediate trapped during turnover of α-$70^{Val\rightarrow Ile}$ MoFe protein. The spectrum for the α-$70^{Val\rightarrow Ile}$ enzyme shows the signal from the $E_4(4H)$ Janus intermediate, $\mathbf{g} = [2.15, 2.007, 1.965]$. The WT enzyme turned over under high partial pressure of N_2 ($P(N_2)$) shows the EPR signal from the $E_4(2N2H)$ intermediate, in which FeMo-co binds a diazene-level product of N_2 binding/reduction, $\mathbf{g} = [2.09, 1.99, 1.97]$. However, WT enzyme freeze-trapped under low $P(N_2)$ turnover with high solution concentration of H_2 (high effective $P(H_2)$, see figure legend and ref 15) shows only traces of the signal from $E_4(2N2H)$, and instead shows an EPR signal of an intermediate with $g_1 = 2.15$, which is indistinguishable from that of $E_4(4H)$ in the MoFe α-$70^{Val\rightarrow Ile}$ variant.[8,10] Closer inspection of the high-$P(N_2)$ signal then shows a trace of the $g_1 = 2.15$ feature, associated with a very low population of this intermediate, confirming its presence under all turnover conditions.

Such a correlation of relative intensities with $P(N_2)$ and effective $P(H_2)$ is as expected if this $g_1 = 2.15$ signal is indeed from WT $E_4(4H)$. In this case its concentration relative to that of $E_4(2N2H)$ is governed by the equilibrium of Figure 3, when, as expected, the forward and reverse steps of the *re*/*oa*

DOI: 10.1021/jacs.6b06362
J. Am. Chem. Soc. 2016, 138, 10674−10683

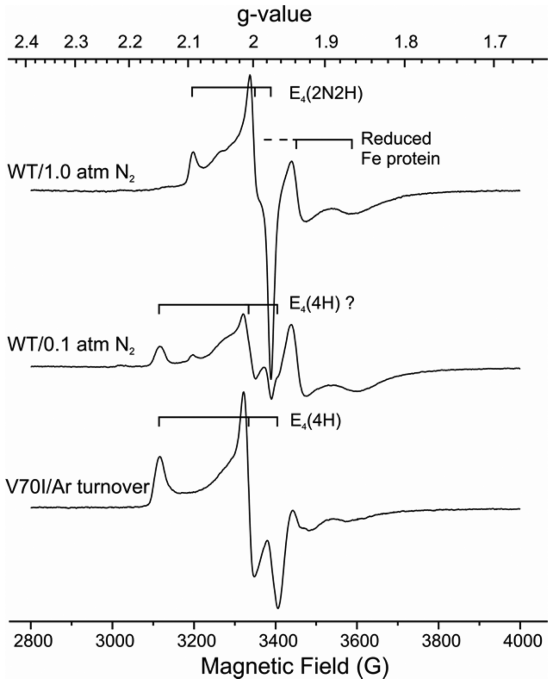

Figure 4. X-band EPR spectra of WT nitrogenase turnover samples trapped under 1 atm of N_2 (with stirring to facilitate transfer of H_2 formed during turnover into the headspace[15]), and under low $P(N_2)$ in H_2O buffer (without stirring) shown in comparison with spectrum of $E_4(4H)$ state trapped during turnover of α-$70^{Val\rightarrow Ile}$ MoFe protein of the same concentration (see Materials and Methods). *EPR conditions*: temperature, 12 K; microwave frequency, 9.36 GHz; microwave power, 10 mW; modulation amplitude, 9 G; time constant, 160 ms; field sweep speed, 20 G/s.

equilibrium are rapid compared to the slow delivery of the next electron from Fe^{red} (Figure 1),

$$\frac{E_4(2N2H)}{E_4(4H)} = K_{re}\frac{P(N_2)}{P(H_2)} \propto P(N_2) \quad (2)$$

Here K_{re} is the equilibrium constant for the *re*/*oa* equilibrium, and a simple proportionality to $P(N_2)$ follows from our observation that at these high enzyme concentrations, turnover produces a roughly constant (saturating) concentration of H_2 regardless of $P(N_2)$.[15] Not only does this $P(N_2)$ dependence supports the idea that the g_1 = 2.15 state is indeed the WT $E_4(4H)$, but of central importance to this study, the ability to prepare samples whose dominant EPR signal is that of the g_1 = 2.15 state enables its characterization and identification, as now described.

^{1,2}H Hyperfine Coupling to Bridging [Fe−H/D−Fe] in WT MoFe. ENDOR spectroscopy revealed the presence in $E_4(4H)$ of α-$70^{Val\rightarrow Ile}$ and α-$70^{Val\rightarrow Ile}$/α-$195^{His\rightarrow Gln}$ MoFe protein of two [Fe−H−Fe] bridging hydrides with anisotropic hyperfine tensors whose principal values are virtually identical, A1 = [11, 25, 37] MHz, A2 = [10, 24, 33] MHz, but whose orientations differ.[8] To begin this investigation, we examined how the hyperfine coupling to the two hydrides influence the EPR spectrum of $E_4(4H)$ of α-$70^{Val\rightarrow Ile}$ MoFe protein. Figure 5A presents CW X-band EPR spectra of this intermediate prepared in H_2O and D_2O buffers, along with expansions of the g_1 and g_3 regions of the spectra plus simulations that incorporate the ENDOR-derived hyperfine couplings to the hydrides/deuterides (the accompanying protons have only

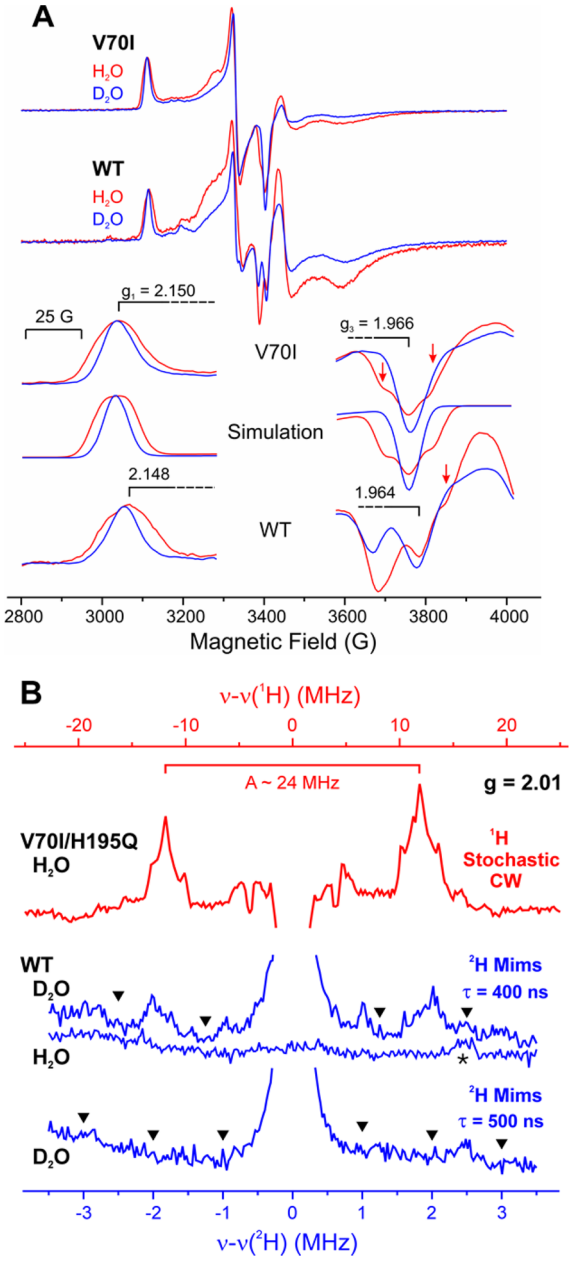

Figure 5. (A) EPR spectra of WT and α-$70^{Val\rightarrow Ile}$ turnover samples trapped in H_2O (red) and D_2O (blue) buffers. Spectra are shown after normalization to the same g_1 feature amplitude and their extended g_1 and g_3 fragments are compared with EPR simulations obtained with hydrides/deuterides hyperfine interaction parameters known from previous ENDOR study.[8] Red arrows indicate resolved features associated with hydrides hyperfine interaction. *EPR conditions*: temperature, 12 K; microwave frequency, 9.36 GHz; microwave power, 10 mW; modulation amplitude, 2.3 G; time constant, 160 ms; field sweep speed,10 G/s; 4 scans. (B) Mims ^{2}H ENDOR spectra of WT low $P(N_2)$ turnover in D_2O (middle) shown in comparison with previously obtained stochastic CW ENDOR of hydrides of $E_4(4H)$ trapped in α-$70^{Val\rightarrow Ile}$/α-$195^{His\rightarrow Gln}$ protein during turnover in H_2O (top).[18] Spectra of ^{2}H and ^{1}H are scaled to the same Larmor frequency. In D_2O spectra, down triangles indicate "blind spots" of Mims ENDOR spectra with suppressed hyperfine couplings of $A = n/\tau$, n = 1, 2, ...; *-labeled signal in the H_2O background Mims τ = 400 ns spectrum is associated with 5th harmonics of the matrix ^{1}H response. *Mims ENDOR conditions*: microwave frequency, 34.743 GHz; $\pi/2$ = 50 ns; RF 20 μs; repetition time 50 ms; ~400−800 scans; temperature, 2 K.

DOI: 10.1021/jacs.6b06362
J. Am. Chem. Soc. 2016, 138, 10674−10683

small couplings and do not significantly contribute). The difference in breadth of the g_1 feature in H_2O and D_2O buffers is well-captured by the simulated ^1H hyperfine broadening from the two hydrides, as calculated using the ENDOR-derived couplings. In particular, at g_3, the EPR spectrum of the intermediate in H_2O buffer even shows the 1−2−1 pattern arising from comparable couplings to the two ^1H hydrides, and this too is reproduced by the simulation. The loss of this pattern in D_2O buffer definitively confirms its identification with coupling to the two hydrides.

The EPR spectrum of the WT g_1 = 2.15 species in H_2O buffer has the same breadth at g_1 = 2.15 as that of $E_4(4H)$ of α-$70^{Val\rightarrow Ile}$, and shows the same narrowing in D_2O. At g_3 the signals from residual Fe^{red} and $E_4(2N2H)$ largely obscure the g_1 = 2.15 intermediate signal for the WT enzyme, but the spectrum in H_2O buffer nonetheless shows clear evidence for the same 1−2−1 hyperfine-coupling pattern from two [Fe−H−Fe] hydrides as seen for the α-$70^{Val\rightarrow Ile}$ variant, a feature that is lost in D_2O buffer as with the α-$70^{Val\rightarrow Ile}$ intermediate. Thus, the WT and α-$70^{Val\rightarrow Ile}$ enzymes have equivalent hyperfine-coupled hydrides.

Comparison of ENDOR responses from $E_4(4H)$ in α-$70^{Val\rightarrow Ile}$ MoFe protein and the g_1 = 2.15 intermediate of WT enzyme confirms the presence of the two bridging hydrides in the WT intermediate. Figure 5B shows a 2 K Q-band stochastic CW ^1H ENDOR spectrum collected at g_2 = 2.01 for $E_4(4H)$ α-$70^{Val\rightarrow Ile}$/α-$195^{His\rightarrow Gln}$.[18] This spectrum is one component of the 2D field-frequency pattern of spectra collected across the EPR envelope used to carry out the ENDOR analysis. In this spectrum, taken at the field of maximum EPR intensity,[8] the strongly coupled ^1H signals from the two hydrides are completely overlapped, yielding a single composite (structured) doublet whose feature of maximum intensity corresponds to a hyperfine splitting, $A(^1H) \sim 24$ MHz.

The population of the g_1 = 2.15 intermediate trapped during turnover of WT enzyme in H_2O buffer is low, even when enhanced by low $P(N_2)$, which prevented collection of a satisfactory ENDOR response for strongly coupled [Fe−^{1}H−Fe] protons. However, during turnover of the WT enzyme in D_2O buffer the intermediate is trapped with a more than 2-fold higher population. As a result, we could obtain ^2H ENDOR signals from strongly coupled [Fe−^{2}H−Fe] deuterons. The Q-band ^2H Mims pulsed-ENDOR spectrum at g = 2.01 shows a narrow "distant deuteron" signal centered at the ^2H Larmor frequency (Figure 5B), but in addition shows a pair of peaks offset from the ^2H Larmor frequency by $\sim \pm 1.85$ MHz. The identification of this pair as a hyperfine-split doublet with $A(^2H) \sim 3.7$ MHz is confirmed by its suppression when the interval, τ, in the Mims microwave pulse sequence is chosen appropriately for the hyperfine coupling, in this case $A(^2H)\tau \sim 2$, and by the absence of the signal in a sample prepared in H_2O buffer, Figure 5B.[19] When scaled by the nuclear g-factors, the coupling for this feature corresponds to a proton coupling of $A(^1H) \sim 24$ MHz, the value seen in the ^1H spectrum from $E_4(4H)$ α-$70^{Val\rightarrow Ile}$/α-$195^{His\rightarrow Gln}$.

Together, the EPR and ENDOR measurements demonstrate that the WT g_1 = 2.15 intermediate not only has the same g-values as α-$70^{Val\rightarrow Ile}$ $E_4(4H)$ (vide supra), but also exhibits hyperfine couplings that correspond to the pair of [Fe−H−Fe] bridging hydrides of α-$70^{Val\rightarrow Ile}$ $E_4(4H)$, *thereby establishing that the intermediate in WT MoFe protein corresponds to that in the* α-$70^{Val\rightarrow Ile}$ *variant: it is the* $E_4(4H)$ *Janus intermediate of* N_2 *reduction by the WT enzyme.*

Photoinduced *re* of WT and α-$70^{Val\rightarrow Ile}$ $E_4(4H)$ Hydrides; *oa* of H_2 by Cryoannealing $E_4(2H)$*. The assignment of the WT g_1 = 2.15 intermediate to $E_4(4H)$, with its two [Fe−H−Fe] bridging hydrides, is confirmed by the behavior of this intermediate under photolysis. We were inspired to take this approach by considering that the photolysis of transition metal dihydride complexes (with mutually *cis* hydride ligands) commonly results in the release of H_2,[20−28] which represents "a typical example of reductive elimination", while the thermal reverse reaction "is the prototype example of an oxidative addition reaction."[20] Thus, we tested whether the two bridging hydrides of $E_4(4H)$ would behave in this fashion.[18] ENDOR and EPR measurements showed that photolysis of $E_4(4H)$ α-$70^{Val\rightarrow Ile}$ at 4 K and above generates a new FeMo-co state, denoted $E_4(2H)$*, through the photoinduced *re* of the two bridging hydrides as H_2. The $E_4(2H)$* thus trapped relaxes to the initial, equilibrium, $E_4(4H)$ form during cryoannealing of the frozen solid at temperatures above 175 K, where the oxidative addition (*oa*) of the eliminated H_2 by $E_4(2H)$* becomes kinetically allowed. The photolysis quantum yield is temperature invariant at liquid helium temperatures and shows a large kinetic isotope effect, KIE ≈ 10. These observations imply the photoinduced release of H_2 involves a barrier to the combination of the two nascent H atoms and further suggest that H_2 formation involves nuclear tunneling through that barrier.

Figure 6 compares EPR signals collected during the in situ irradiation by 450 nm light of $E_4(4H)$ α-$70^{Val\rightarrow Ile}$, WT $E_4(4H)$,

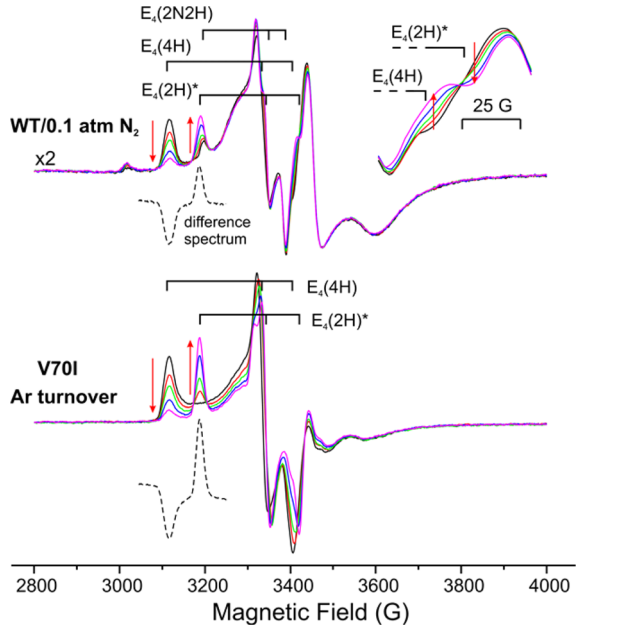

Figure 6. Photoinduced changes in EPR spectra of WT and α-$70^{Val\rightarrow Ile}$ freeze-trapped during enzymatic turnover in H_2O during 24.5 min of 450 nm diode laser irradiation at 12 K. *EPR conditions*: the same as in Figure 4.

and $E_4(2N2H)$ held at 12 K in an EPR cavity. Figure 7A plots the time course for the intensity of the EPR signals of these intermediates during the in situ photolysis. Irradiation converts $E_4(4H)$ α-$70^{Val\rightarrow Ile}$ (**g** = [2.15, 2.007, 1.965]) to $E_4(2H)$* (**g** = [2.098, 2.0, 1.956]), Figure 6. The figure shows that irradiation of WT $E_4(4H)$ likewise converts this state to an $E_4(2H)$* state with g-values identical to those in the α-$70^{Val\rightarrow Ile}$ MoFe variant.

DOI: 10.1021/jacs.6b06362
J. Am. Chem. Soc. 2016, 138, 10674−10683

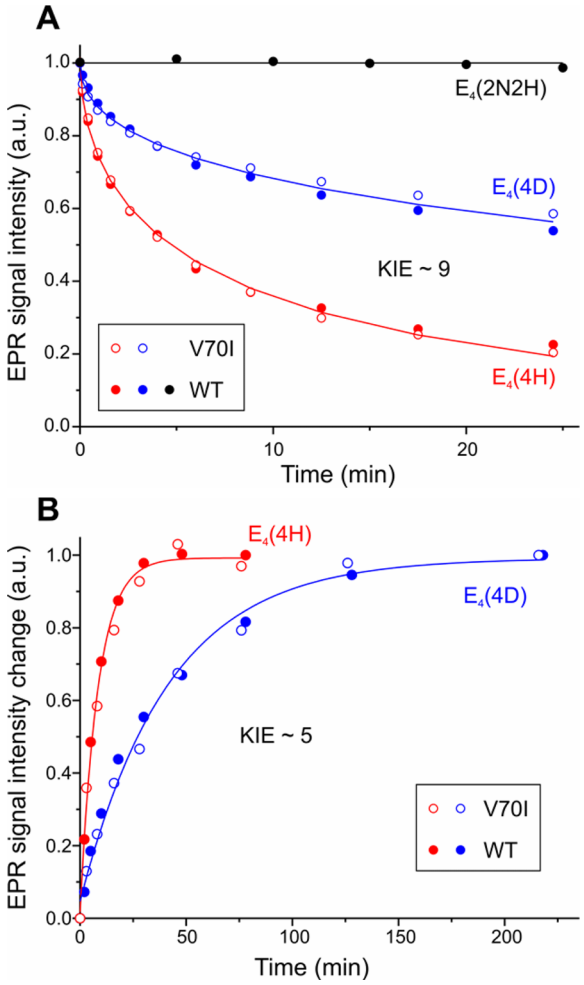

Figure 7. (A) Time courses of $E_4(4H)$ and $E_4(4D)$ states in α-$70^{Val\rightarrow Ile}$ and WT and $E_4(2N2H)$ in WT 1 atm N_2 turnover in H_2O during irradiation with 450 nm diode laser at 12 K. Data points in this and following kinetics plots were obtained as described in Materials and Methods; decays of $E_4(4H)$ and $E_4(4D)$ are fitted as stretched exponential with following parameters: τ = 9.2 min, m = 0.51 for H_2O and τ = 83.3 min, m = 0.45 for D_2O. *EPR conditions*: for this and the following kinetics figures are the same as in Figure 4. (B) Time courses of $E_4(4H)$/ $E_4(4D)$ recovery during 193 K annealing of irradiated WT and α-$70^{Val\rightarrow Ile}$ turnovers in H_2O/D_2O. Time constants obtained from exponential fit: 8.4 min (H_2O) and 41.5 min (D_2O), KIE ~ 5.

In contrast, the EPR spectra of Figure 6 and progress curves of Figure 7A, show that the $E_4(2N2H)$ signal is unaffected by photolysis. That a bound nitrogenous moiety, the N_2-derived 2N2H moiety of $E_4(2N2H)$, is not photodissociable supports the idea that the photosensitivity is associated with the presence of bound hydrides. *The photolyis results thus confirm the presence of the two bridging hydrides in the WT g_1 = 2.15 intermediate, and its identification as $E_4(4H)$.*

The progress curves for in situ irradiation of $E_4(4H)$ in WT and α-$70^{Val\rightarrow Ile}$ MoFe protein (Figure 7A) are the same, within error, showing that the quantum yield for *re* of H_2 is independent of environment: WT enzyme vs α-$70^{Val\rightarrow Ile}$ variant. As a result, the *re* progress curves for WT and α-$70^{Val\rightarrow Ile}$ in H_2O buffer have been jointly fit to the stretched exponential behavior $(\exp(-(t/\tau)^m))$[29,30] that is a consequence of photolysis in a nonglassy sample,[18] and likewise for those in D_2O buffer. As reported for photolysis of $E_4(4H)$ α-$70^{Val\rightarrow Ile}$, the joint progress curves show a large KIE, defined as the ratio of the median decay times for D_2O and H_2O buffers, KIE ~ 9, which implies that photoinduced *re* of the two hydrides and release of H_2 involves a barrier to the combination of the two nascent H atoms. Likewise, as reported for the α-$70^{Val\rightarrow Ile}$ intermediate, the decay time for the WT intermediate is temperature invariant, within error, for T = 4−12 K, which suggests that the formation of H_2 involves nuclear tunneling through that barrier.[31]

Figure 7B plots the timecourse for the *oa* of H_2 by the $E_4(2H)^*$ and $E_4(2D)^*$ to regenerate the corresponding $E_4(4H)/E_4(4D)$ states during 193 K cryoannealing of WT and α-$70^{Val\rightarrow Ile}$ MoFe samples.[18] In these experiments the sample is annealed at 193 K multiple times, with cooling for collection of EPR spectra at 12 K between annealing periods. For both H_2O and D_2O buffers the relaxation of $E_4(2H)^*$ *oa* of H_2 regenerates the $E_4(4H)$ state formed during turnover, and the progress curves are well-fitted as a single-exponential processes. As with photoinduced *re*, the progress curves during cryoannealing *oa* are the same for the two MoFe variants, and their joint fit yields KIE ~ 5, rather larger than seen for closed-shell monometallic complexes.[32,33] Combined with a strong temperature dependence of the time-constant (not shown), this KIE implies that *oa* of H_2 involves traversal of an energy barrier.

Overall, the measurements of photoinduced, *re* loss of H_2 from $E_4(4H)$ and thermal regeneration of the $E_4(4H)$ state via *oa* of H_2 by the resulting $E_4(2H)^*$ confirm the identification of the WT and α-$70^{Val\rightarrow Ile}$ intermediates as the same Janus, in showing that both the excited and ground state energy surfaces associated with these processes are essentially the same in the WT and variant MoFe proteins.

Accumulation of $E_4(4H)$ Isotopologues During Mixed-Isotope Turnover; Bridging Hydrides Are Exchange-Inert. The kinetic reversibility of the *re*/*oa* mechanism in WT enzyme, as well as the stability of the bridging hydrides to solvent exchange, as required by *Key Constraint* (ii)b, Chart 1, are here established by the use of EPR and photolysis to measure the isotopic composition of the bridging hydrides in WT Janus trapped during N_2 turnover under isotopically mixed conditions: H_2O buffer under an atmosphere that include D_2 and conversely, Figure 8. These measurements show that the *re*/*oa* mechanism satisfies *Key Constraints*, Chart 1, on catalysis by WT nitrogenase.

According to the *re*/*oa* mechanism, N_2 turnover in H_2O buffer under D_2 would generate $E_4(4H)$ through turnover accumulation of reducing equivalents and protons derived from solvent (Figure 1), but in addition, *oa* of D_2 from the gas phase by $E_4(2N2H)$ would generate $E_4(2D^-;2H^+)$, with two [Fe−D−Fe] bridges and two bound protons, and conversely for turnover in D_2O buffer under H_2 (Figure 3). As a result, during N_2 turnover under both mixed-isotope conditions, two isotopologues of Janus are expected to accumulate, one in which the two bridges have the solvent H/D isotope, the other with the two bridges generated through *oa* of the diatomic D_2/H_2 in the gas phase.[14]

Figure 8A shows that the g_1 = 2.15 feature from the EPR spectrum of the WT $E_4(4H)$ intermediate, as trapped in H_2O buffer during turnover under N_2/D_2, is distinctly narrower than for turnover under N_2/H_2, thus demonstrating the accumulation of an intermediate in which the reverse of the *re*/*oa* equilibrium has generated [Fe−D−Fe] bridging deuterides with loss of the ^1H hyperfine broadening (Figure 5A, above). Conversely the g_1 = 2.15 feature for the WT Janus intermediate in D_2O buffer is correspondingly broader for turnover under

DOI: 10.1021/jacs.6b06362
J. Am. Chem. Soc. 2016, 138, 10674−10683

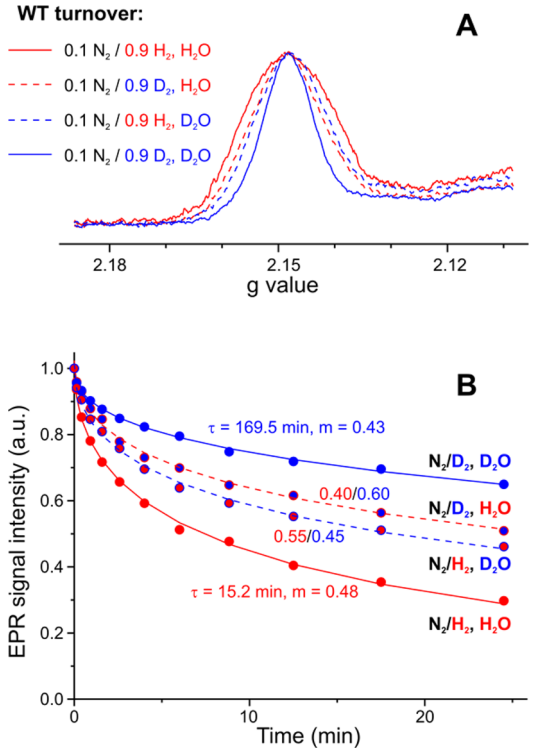

Figure 8. (A) The g_1 features of Janus state EPR recorded for WT protein turnovers trapped under mixtures of 0.1 atm N_2 with 0.9 atm of H_2 or D_2 in H_2O and D_2O buffers with stirring. *EPR conditions*: temperature, 12 K; microwave frequency, ∼ 9.36 GHz; microwave power, 10 mW; modulation amplitude, 4.5 G; time constant, 160 ms; field sweep speed, 5 G/s; 4−8 scans. (B) Photolysis of WT Janus intermediate formed through isotopically mixed turnover; irradiation with 450 nm light at 12 K. Progress curves for N_2/H_2, H_2O and N_2/D_2, D_2O are fitted as stretched exponential decays with parameters shown in the figure. Kinetics of other two samples can be well fitted with following parameters: τ = 52.6 min, m = 0.47 for N_2/D_2 turnover in H_2O and τ = 38.3 min, m = 0.46 for N_2/H_2 turnover in D_2O. Dotted lines present alternative fits as sums of two decays corresponding to photolysis of $E_4(4H)$ in H_2O and $E_4(4D)$ in D_2O turnover samples with ratios shown in the figure.

N_2/H_2 than for turnover under N_2/D_2, demonstrating the accumulation of an intermediate with bridging [Fe−H−Fe], which contribute ^1H hyperfine broadening. Simulations that sum roughly equal contributions of the limiting spectra for $E_4(4H)$ and $E_4(4D)$ in fact reproduce the mixed-isotope spectrum quite well (not shown). *Note especially*, that the demonstration that deuterides/hydrides acquired by *oa* of the gas-phase diatomic accumulate in the catalytic intermediate, rather than exchanging with a solvent of opposite isotopic composition, confirms our proposal[6,7] that these bridging hydrides are exchange-inert, and that their formation during *oa* of a gas-phase diatomic explains why turnover under N_2/T_2 does not lead to the exchange of T^+ into the solvent.[2]

The accumulation of mixtures of $E_4(4H)$ isotopologues during turnover by *oa* of H_2/D_2 under isotopically mixed conditions is actually seen most dramatically when comparing measurements of the KIE for the photolysis of WT Janus trapped during turnover under N_2 in isotopically homogeneous conditions—H_2O buffer with addition of 0.9 atm of H_2, or D_2O buffer with added D_2—with those for isotopically mixed turnover conditions—H_2O buffer with added D_2 or D_2O buffer with added H_2. As expected, the photolysis traces from isotopically homogeneous intermediates, formed in H_2O buffer with N_2/H_2 and in D_2O buffer with N_2/D_2, Figure 8B, show a large KIE ∼ 11, within error the same as seen for *re* of the two hydrides/deuterides formed in H_2O/D_2O buffers without the diatomics in the atmosphere (Figure 7A).

However, according to the *re*/*oa* mechanism, *oa* of D_2 by $E_4(2N2H)$ during turnover in H_2O buffer under D_2 generates $E_4(2D^-;2H^+)$, with two [Fe−D−Fe] bridges and two bound protons, and conversely for turnover in D_2O buffer under H_2. To a good approximation each of these $E_4(4H)$ mixed isotopologues should undergo photoinduced *re* with quantum yield associated with the isotopic composition of the bridges, as determined by the complementary diatomic (see above), independent of the isotopic character of the protons/deuterons on sulfur, as determined by the solvent. Thus, if the H/D bridges introduced from the diatomic do not exchange with solvent, the intermediates formed in mixed isotope turnover should have apparent rates of photolysis roughly midway between those of $E_4(4H)$ and $E_4(4D)$. Indeed, Figure 8B shows that the Janus intermediate formed during turnover under N_2/D_2 in H_2O buffer photolyzes more slowly than with N_2/H_2 in H_2O, while the intermediate formed under N_2/H_2 in D_2O buffer photolyzes more rapidly than with N_2/D_2 in D_2O. The photolysis of these mixed-isotope samples each can be described by time constant roughly midway between those of the two isotopically homogeneous samples (see figure legend). Alternatively, as shown in Figure 8B, each isotopically mixed trace can be fit as the sum of a roughly f ∼ 50% contribution from the progress curve for photolysis of $E_4(4H)$, with two bridging hydrides, plus a contribution of $(1 - f)$ from the curve for $E_4(4D)$ with two bridging deuterides.[34]

These EPR and photochemical observations thus confirm that turnover of WT MoFe protein under N_2 involves a rapidly reversible *re*/*oa* equilibrium between the E_4 Janus intermediate and the E_4 state with diazene-level dinitrogen reduction product, Figure 3. Furthermore, the buildup of $E_4(2D^-;2H^+)$ with bridging deuterides during N_2/D_2 turnover in H_2O buffer, and the converse, confirm that the bridging hydrides/deuterides of the Janus intermediate do not exchange with solvent during turnover. Thus, these measurements show that the *re*/*oa* mechanism indeed satisfies *Key Constraints* (i), (ii)b,c, Chart 1, as proposed.[6,7]

Kinetic Reversibility of the *re*/*oa* Equilibrium during N_2 Reduction by WT MoFe. The $E_4(4H)$ α-$70^{Val\rightarrow Ile}$ intermediate was shown to have accumulated four reducing equivalents by a quench-cryoannealing relaxation protocol corresponding to that described above for the regeneration of $E_4(4H)$ by *oa* of H_2 to the photogenerated $E_4(2H)$*. Keeping the sample frozen prevents any additional accumulation of reducing equivalents because binding of reduced Fe protein to and release of oxidized protein from the MoFe protein both are abolished in a frozen solid. As recently confirmed,[35] the frozen intermediate can relax toward the resting state only through steps that release a stable species from FeMo-co, with the E_n states formed prior to N_2 binding losing 2 equiv per relaxation step in the release of H_2. By this approach, $E_4(4H)$ was identified by its relaxation to the resting state E_0 through the release of a total of four reducing equivalents in a two-step process, each step involving hydride protonation with release of H_2 (2 equiv per step), with formation of $E_2(2H)$ in the first step (Figure 1).[10]

As an extension of this procedure, the FeMo-co S = 1/2 $E_4(2N2H)$ intermediate trapped during catalytic turnover of

DOI: 10.1021/jacs.6b06362
J. Am. Chem. Soc. 2016, 138, 10674−10683

WT enzyme was identified by the finding that the decay of this state in a frozen reaction mixture is accelerated by increasing $[H_2]$ and slowed by increasing $[N_2]$, which directly demonstrated that the intermediate is the product of the kinetically, as well as thermodynamically reversible (*re*/*oa*) activation equilibrium, Figure 3.[15] However, in that study the $E_4(4H)$ precursor to *re* was accumulated in such low levels that its kinetic progress curve during cryoannealing could not be monitored directly, and we were forced to analyze the decay of $E_4(2N2H)$ to resting state, Chart 3, through a steady-state approximation for the concentration of $E_4(4H)$.

Chart 3

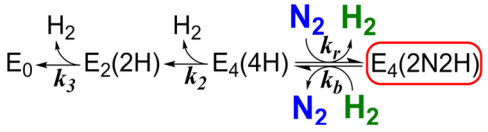

The preparation of freeze-quenched WT samples that contain significant populations of both $E_4(4H)$ and $E_4(2N2H)$, obtained through control of $P(N_2)$ during turnover, has now enabled us to directly monitor the progress curves in WT enzyme of all LT species on the cryoannealing relaxation pathway of $E_4(2N2H)$ to resting state (E_n states with $n \leq 4$, even), Chart 3. In so doing we directly track the kinetics of the species linked through the *oa* reverse of the *re*/*oa* equilibrium, Figures 1, 3. These progress curves for the relaxation of $E_4(2N2H)$ and kinetically linked intermediates (Chart 3) during cryoannealing of WT enzyme at −50 °C are presented in Figure 9. These are well described by the curves calculated by fitting them to the sequential kinetic scheme of Figure 9, which corresponds to the reverse of the LT scheme starting at $E_4(2N2H)$, Figure 1 and Chart 3. The fitting procedure allowed for each step to exhibit distributed kinetics, and the time-constants and "stretch" parameters are collected in the legend to Figure 9. The amplitudes of the kinetic phases correspond to the steady-state turnover populations of the E_n states, and of course vary widely depending on $P(N_2)$ and the electron flux (see Figure 4). In the sample represented by Figure 9 these correspond to $E_0 \sim 8\%$; $E_2 \sim 16\%$; $E_4(4H) \sim 8\%$; $E_4(2N2H) \sim 12\%$. Thus, in this sample the two states linked by the *re*/*oa* equilibrium correspond to fully ∼20% of the MoFe protein. The remainder of the MoFe protein is in EPR-silent E_n, n = *odd* states, ∼ 56%; these cannot relax to E_0 during cryoannealing.[35]

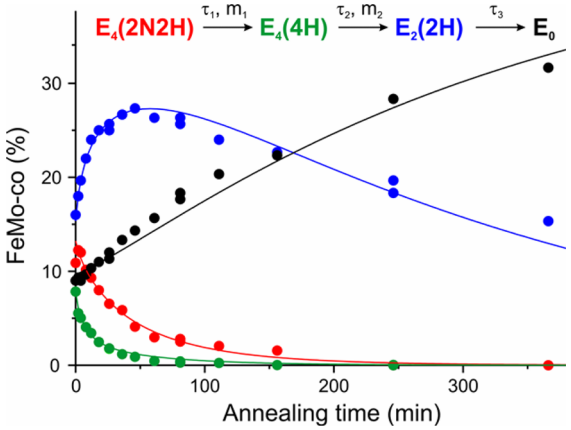

Figure 9. Time courses of four EPR detected states during −50 °C cryoannealing of WT low $P(N_2) \sim 0.05$ atm turnover in H_2O. The data colors correspond to those in the kinetic scheme (top) and the lines correspond to fits to that scheme as previously described.[10] Stretched exponential parameters of the first two fast steps are $\tau_1 = 43$ min, $m_1 = 0.79$ and $\tau_2 = 6$ min, $m_2 = 0.8$, the third slow step fitted as exponential with $\tau_3 = 330$ min. Intensities of E_2 and E_0 states obtained and quantitated with previously described procedures;[15] intensities of E_4 states converted to concentration units by scaling three-step kinetic scheme for corresponding decays. *EPR conditions*: for $E_4(4H)$ spectra the same as in Figure 4; for $E_4(2N2H)$, E_2 and E_0 the same as used in previous studies.[15]

The kinetic coupling of the loss of $E_4(2N2H)$ through *oa* of H_2, with the formation of $E_4(4H)$ directly establishes the operation of the *re*/*oa* mechanism and its kinetic reversibility. The above demonstration that *oa* of D_2 by $E_4(2N2H)$ in H_2O yields $E_4(2D^-;2H^+)$ with exchange-inert deuteride bridges then shows that in this case each of the two steps by which this WT mixed-isotope intermediate relaxes to E_0 would involve protonation of the deuteride bridges by protons from solvent, generating 2HD, confirming that the *re*/*oa* mechanism explains the final *Key Constraint* (ii)a, Chart 1, as proposed.[6,7]

Thermodynamic Reversibility of the *re*/*oa* Equilibrium during N_2 Reduction by WT MoFe. The mere observation of both $E_4(4H)$ and $E_4(2N2H)$ in samples freeze-quenched during N_2 fixation (Figure 4) establishes that the equilibrium constant for *re*/*oa*, $K_{re} = k_r/k_b$ (Figure 3; Chart 3), is small. The cryoannealing experiments only give k_b, not k_r, but as a rough quantitative estimate of K_{re}, we assign the relative concentrations of $E_4(2N2H)$ and $E_4(4H)$ during turnover under low N_2 partial pressure to the zero-time values determined by the fit to the annealing kinetics (Figure 9), $E_4(2N2H)/E_4(4H) \sim 3/2$, in keeping with the conclusion (vide supra) that the forward and reverse steps of the *re*/*oa* equilibrium are rapid compared to other steps in the catalytic cycle (Figure 1). In this case we can rewrite eq 2 to approximate K_{re} as

$$K_{re} = \frac{E_4(2N2H)}{E_4(4H)} * \frac{P(H_2)}{P(N_2)} \tag{3}$$

The N_2 partial pressure is fixed by the experimental conditions; earlier observations suggest that saturating concentrations of H_2 are formed during turnover under all $P(N_2)$, which suggests an effective $P(H_2) \sim 1$ atm.[15] As a result, one obtains:

$$K_{re} \sim \left(\sim \frac{3}{2} \right) * \left(\frac{\sim 1}{0.05} \right) \sim 30 \tag{4}$$

$$\Delta_{re}G^{\circ} = -RT \ln(K_{re}) \sim -2 \text{ kcal/mol} \tag{5}$$

The LT kinetic measurements likewise yielded values for the *re* process: $K_{re} \sim 0.7$ and $\Delta_{re}G^0 \sim +0.2$ kcal/mol.[2,4] Given the difference in methodologies—direct observation of species in equilibrium in the present study, analysis of turnover kinetics in the former—and the differences in origin of the MoFe proteins—*Azotobacter vinelandii* in the present study and *Klebsiella pneumoniae* in the former—we consider the measurements to be in excellent agreement: *nitrogenase catalysis, driven by the re of H_2, turns the highly endothermic first step in the reduction of the N_2 triple bond, (to the diazene level) into the essentially thermoneutral re/oa equilibrium conversion of* Figure 3.

CONCLUSIONS

The *re*/*oa* mechanism for N_2 reduction by nitrogenase postulates that the reduction of the N_2 triple bond to a

DOI: 10.1021/jacs.6b06362
J. Am. Chem. Soc. 2016, 138, 10674−10683

2N2H (diazene) level is driven by the obligatory formation of one H_2 for each N_2 reduced. This proposal was based on identification of a FeMo-co $S = 1/2$ state trapped during turnover of the α-$70^{Val\rightarrow Ile}$ MoFe protein as the Janus intermediate: the $E_4(4H)$ state, which stores four reducing equivalents as two [Fe−H−Fe] bridging hydrides. Once this identification is made, then the LT $E_4(4H) \leftrightarrow E_4(2N2H)$ equilibrium (Figure 1) ceases to be a "mystery": the connection with the organometallic chemistry of metal-dihydride complexes identifies this process as the mechanistically coupled reductive elimination (*re*) of H_2 (Figure 3). The H_2 formed during *re* carries away two of the four reducing equivalents stored in $E_4(4H)$ and drives the reaction, while the metal-ion core of FeMo-co becomes activated to reduce N_2 through the simultaneous acquisition of two reducing equivalents. The mechanism was first supported by its proposed explanation of the *Key Constraints* of Chart 1, and then two new predictions regarding turnover by WT MoFe were promptly verified,[14,15] adding direct experimental support.

As we now summarize, the present report establishes the presence of Janus in WT enzyme, its participation in N_2 reduction, and the operation of the *re*/*oa* equilibrium during N_2 reduction. Experiments *on WT enzyme* further show that this mechanism satisfies all the *Key Constraints* imposed on N_2 reduction by decades of careful study by others summarized in Chart 1[2] and that the *re*/*oa* equilibrium in WT MoFe is indeed kinetically and thermodynamically reversible, thereby establishing the role of the *re*/*oa* equilibrium in N_2 reduction (Figure 3).[6,7]

(i) EPR/ENDOR, and photophysical measurements establish that the intermediate with $g_1 = 2.15$ trapped during nitrogen fixation by WT MoFe in fact is the $E_4(4H)$ Janus intermediate of N_2 reduction, which has accumulated four reducing equivalents stored as [Fe−H−Fe] bridging hydrides, whose properties are identical to those of the Janus intermediate first trapped in the α-$70^{Val\rightarrow Ile}$ MoFe variant. This observation thereby establishes the freeze-trapped α-$70^{Val\rightarrow Ile}$ Janus intermediate as a reliable guide to mechanism, *but most importantly, enables direct observation of the participation of the Janus intermediate in N_2 reduction and the re/oa process during catalysis by the WT enzyme. The new findings and conclusions that build on this foundation are summarized next.*

(ii) Examination of the isotopic composition of WT Janus during turnover in H_2O buffer under D_2 (or D_2O buffer under H_2) establishes that *oa* of D_2 from the gas phase by $E_4(2N2H)$ accumulates $E_4(2D^-;2H^+)$, with two [Fe−D−Fe] bridges and two bound protons from solvent (or $E_4(2H^-;2D^+)$) (Figure 3), and that the bridging hydrides/deuterides do not exchange with solvent during turnover. This demonstrates experimentally that the *re*/*oa* mechanism accounts for the longstanding *Key Constraints* on mechanism, Chart 1, (i), (ii)b,c.

(iii) The observation and successful modeling of the entire relaxation pathway of WT enzyme by which $E_4(2N2H)$ relaxes to the resting-state, E_0, including the *oa* of H_2, to form Janus with release of N_2, and two subsequent steps of hydride protonation each with release of H_2, Figure 1, eq 2, demonstrates the kinetic reversibility of the *re*/*oa* equilibrium, Figure 3, Chart 3, and shows that *re*/*oa* satisfies the last of the *Key Constraints*, (ii)a, in addition to confirming that it satisfies (ii)c.

(iv) An estimate of the free energy for the *re* of H_2 by FeMo-co that has accumulated four reducing equivalents, with reduction of N_2 to generate a 2N2H-level species (Figure 3) in WT enzyme, quantifies the thermodynamic reversibility of the first step in the reduction of N_2 by nitrogenase: this reaction is essentially thermoneutral, $\Delta_{re}G^0 \sim -2$ kcal/mol, whereas direct hydrogenation of gas-phase N_2 is highly endergonic.[16]

In summary, in this report we have described the central mechanistic steps by which the WT nitrogenase carries out one of the most challenging chemical transformation in biology, the reduction of the N≡N triple bond.

AUTHOR INFORMATION

Corresponding Authors

*bmh@northwestern.edu

*lance.seefeldt@usu.edu

Notes

The authors declare no competing financial interest.

ACKNOWLEDGMENTS

This work was funded by the NIH (GM 111097; BMH), NSF (MCB 1515981 to BMH) and U.S. Department of Energy; Office of Science, Basic Energy Sciences (BES) (DE-SC0010687 and DE-SC0010834; LCS and DRD).

REFERENCES

(1) Smil, V. *Enriching the Earth: Fritz Haber, Carl Bosch, and the Transformation of World Food Production*; MIT Press: Cambridge, MA, 2001.

(2) Burgess, B. K.; Lowe, D. J. *Chem. Rev.* **1996**, *96*, 2983.

(3) Thorneley, R. N. F.; Lowe, D. J. *Met. Ions Biol.* **1985**, *7*, 221.

(4) Wilson, P. E.; Nyborg, A. C.; Watt, G. D. *Biophys. Chem.* **2001**, *91*, 281.

(5) Simpson, F. B.; Burris, R. H. *Science* **1984**, *224*, 1095.

(6) Hoffman, B. M.; Lukoyanov, D.; Yang, Z. Y.; Dean, D. R.; Seefeldt, L. C. *Chem. Rev.* **2014**, *114*, 4041.

(7) Hoffman, B. M.; Lukoyanov, D.; Dean, D. R.; Seefeldt, L. C. *Acc. Chem. Res.* **2013**, *46*, 587.

(8) Igarashi, R. Y.; Laryukhin, M.; Dos Santos, P. C.; Lee, H. I.; Dean, D. R.; Seefeldt, L. C.; Hoffman, B. M. *J. Am. Chem. Soc.* **2005**, *127*, 6231.

(9) Lukoyanov, D.; Yang, Z.-Y.; Dean, D. R.; Seefeldt, L. C.; Hoffman, B. M. *J. Am. Chem. Soc.* **2010**, *132*, 2526.

(10) Lukoyanov, D.; Barney, B. M.; Dean, D. R.; Seefeldt, L. C.; Hoffman, B. M. *Proc. Natl. Acad. Sci. U. S. A.* **2007**, *104*, 1451.

(11) Hartwig, J. *Organotransition Metal Chemistry: From Bonding to Catalysis*; University Science Books: Sausalito, CA, 2010.

(12) Crabtree, R. H. *The Organometallic Chemistry of the Transition Metals*, 5th ed.; Wiley: Hoboken, NJ, 2009.

(13) Peruzzini, M., Poli, R., Eds.; *Recent Advances in Hydride Chemistry*; Elsevier Science B.V.: Amsterdam, Netherlands, 2001.

(14) Yang, Z.-Y.; Khadka, N.; Lukoyanov, D.; Hoffman Brian, M.; Dean Dennis, R.; Seefeldt Lance, C. *Proc. Natl. Acad. Sci. U. S. A.* **2013**, *110*, 16327.

(15) Lukoyanov, D.; Yang, Z. Y.; Khadka, N.; Dean, D. R.; Seefeldt, L. C.; Hoffman, B. M. *J. Am. Chem. Soc.* **2015**, *137*, 3610.

(16) $\Delta_rG^0[H_2(g) + XY(g) \rightarrow H_2XY(g)]$; N_2, ~ +50 kcal/mol; CO, ~ +4 kcal/mol.

(17) Christiansen, J.; Goodwin, P. J.; Lanzilotta, W. N.; Seefeldt, L. C.; Dean, D. R. *Biochemistry* **1998**, *37*, 12611.

(18) Lukoyanov, D.; Khadka, N.; Yang, Z. Y.; Dean, D. R.; Seefeldt, L. C.; Hoffman, B. M. *J. Am. Chem. Soc.* **2016**, *138*, 1320.

(19) Schweiger, A.; Jeschke, G. *Principles of Pulse Electron Paramagnetic Resonance*; Oxford University Press: Oxford, U.K., 2001.

(20) Perutz, R. N. *Pure Appl. Chem.* **1998**, *70*, 2211.

DOI: 10.1021/jacs.6b06362
J. Am. Chem. Soc. 2016, 138, 10674−10683

(21) Colombo, M.; George, M. W.; Moore, J. N.; Pattison, D. I.; Perutz, R. N.; Virrels, I. G.; Ye, T. Q. *J. Chem. Soc., Dalton Trans.* **1997**, 2857.
(22) Whittlesey, M. K.; Mawby, R. J.; Osman, R.; Perutz, R. N.; Field, L. D.; Wilkinson, M. P.; George, M. W. *J. Am. Chem. Soc.* **1993**, *115*, 8627.
(23) Ballmann, J.; Munha, R. F.; Fryzuk, M. D. *Chem. Commun.* **2010**, *46*, 1013.
(24) Ozin, G. A.; Mccaffrey, J. G. *J. Phys. Chem.* **1984**, *88*, 645.
(25) Dugan, T. R.; Holland, P. L. *J. Organomet. Chem.* **2009**, *694*, 2825.
(26) Yu, Y.; Smith, J. M.; Flaschenriem, C. J.; Holland, P. L. *Inorg. Chem.* **2006**, *45*, 5742.
(27) Smith, J. M.; Sadique, A. R.; Cundari, T. R.; Rodgers, K. R.; Lukat-Rodgers, G.; Lachicotte, R. J.; Flaschenriem, C. J.; Vela, J.; Holland, P. L. *J. Am. Chem. Soc.* **2006**, *128*, 756.
(28) Yu, Y.; Sadique, A. R.; Smith, J. M.; Dugan, T. R.; Cowley, R. E.; Brennessel, W. W.; Flaschenriem, C. J.; Bill, E.; Cundari, T. R.; Holland, P. L. *J. Am. Chem. Soc.* **2008**, *130*, 6624.
(29) Phillips, J. C. *Rep. Prog. Phys.* **1996**, *59*, 1133.
(30) Berberan-Santos, M. N.; Bodunov, E. N.; Valeur, B. *Chem. Phys.* **2005**, *315*, 171.
(31) Work in progress suggests the process involves initial formation of an H2 complex.
(32) Abu-Hasanayn, F.; Goldman, A. S.; Krogh-Jespersen, K. *J. Phys. Chem.* **1993**, *97*, 5890.
(33) Campian, M. V.; Perutz, R. N.; Procacci, B.; Thatcher, R. J.; Torres, O.; Whitwood, A. C. *J. Am. Chem. Soc.* **2012**, *134*, 3480.
(34) We are aware that this partitioning is simplified in that it does not consider other isotopologues that may be formed during steady-state turnover.
(35) Lukoyanov, D.; Yang, Z. Y.; Duval, S.; Danyal, K.; Dean, D. R.; Seefeldt, L. C.; Hoffman, B. M. *Inorg. Chem.* **2014**, *53*, 3688.

DOI: 10.1021/jacs.6b06362
J. Am. Chem. Soc. 2016, 138, 10674−10683